Integrated Waveguide Absorbance Optode for Chemical Sensing

ARTICLE *in* ANALYTICAL CHEMISTRY · JUNE 2013

Impact Factor: 5.64 · DOI: 10.1021/ac990156l

Anal. Chem. **1999,** *71,* 5037−5044

Integrated Waveguide Absorbance Optode for Chemical Sensing

Mar Puyol, Manuel del Valle, Ignacio Garcés,[†] Francisco Villuendas,[‡] Carlos Domínguez,[§] and Julian Alonso*

Sensors & Biosensors Group, Department of Chemistry, Autonomous University of Barcelona, Edifici Cn, 08193 Bellaterra, Catalonia, Spain

A new type of absorbance-based optical sensor is presented. It is based on a chemical transduction membrane that acts simultaneously as the sensing element and as the light guiding medium. This membrane is inserted between two micromachined waveguides in a silica on silicon structure. Light propagates longitudinally through the membrane, which changes its spectral properties accordingly while interacting with the analyte. As the path length corresponds to the membrane length, not its thickness, high sensitivity can be achieved without an increase of the response time. This paper summarizes the design, the construction, and the validation results obtained with integrated waveguide absorbance optode (IWAO) prototypes. The main advantages of the reported optode are its simple configuration, high sensitivity, and versatility. Experimental results obtained with this IWAO, using a potassium-selective bulk optode, are shown and compared to those obtained with a conventional absorbance device incorporating the same membrane. The optimum membrane thickness of 4 μm gave the lowest light losses (15 dB). The absorbance sensitivities obtained (−0.86 AU/decade) were, as expected, higher than those shown by the conventional device (−0.03 AU/decade), with comparable response times ($t_{90\%}$ = 0.5 min).

Interest in optical sensor development has been growing rapidly in recent years. This fact is related to the potential advantages of joining optical transduction, which gathers an ample basis on the analytical knowledge of absorbance or fluorescence techniques, with the technological improvements attained by the telecommunication industry in the field of optical information transmission. For this reason, new research in this field is aimed at the development of light guided optical sensors using cylindrical (optical fibers) and planar waveguides. Cylindrical waveguides show some interesting features because they allow measurements at large distances and are capable of reaching places hard to access for the in situ monitoring of environmental[1] or medical[2−6] parameters. On the other hand, planar waveguides represent practically the same concept as optical fibers but in a microfabricated planar design. In short, they present advantages such as miniaturization, easy membrane deposition, and a compatible design with the IC microelectronic technology. In conclusion, the conjugation of both kinds of waveguide supports will provide optochemical sensors with an enhanced performance.

Until now, most of the described miniaturized devices have been based on surface plasmon resonance[7] phenomena or interferometry.[8,9] However, they present poor specificity in the response and instabilities due to temperature or pressure variations. More specific optical sensors are those based on measurement principles such as absorption spectrometry,[10] fluorometry,[11−14] reflectance,[15,16] or evanescent wave spectroscopy.[17]

From the trasduction point of view, the optical phenomena that provide sensing in a waveguide configuration may occur in the core layer or outside it. Despite the fact that the former is the more sensitive one because the sensing area is probed by the major part of the energy, in most optical sensors the sensing region is located in the cladding and is probed by the evanescent field. This kind of sensor requires long interaction distances or a great amount of field out of the waveguide, which in turn makes the response very dependent on variations of the real part of the refractive index.

[†] Current address: Dpto. Ingeniería Electrónica y Comunicaciones, Universidad de Zaragoza, CPS, María de Luna 3, 50015 Zaragoza, Spain.

[‡] Current address: Dpto. Física Aplicada, Universidad de Zaragoza, Spain.

[§] Current address: Centro Nacional de Microelectrónica, 08193 Bellaterra, Catalonia, Spain.

(1) West, S. J.; Ozawa, S.; Seiler, K.; Tan, S. S. S.; Simon, W. *Anal. Chem*. **1992**, *64*, 533−540.
(2) Seiler, K.; Wang, K.; Kuratli, M.; Simon, W. *Anal. Chim. Acta* **1991**, *244*, 151−160.
(3) Peterson, J. I.; Goldstein, S. R.; Fitzgerald, R. V. *Anal. Chem*. **1980**, *52*, 864−869.
(4) Warner, M. D. *Anal. Chem*. **1986**, *58*, 874A−876A.
(5) Wolthuis, R. A.; McCrae, D.; Hartl, J. C.; Saaski, E.; Mitchell, G. L.; Garcin, K.; Willard, R. *IEEE Trans. Biomed. Eng.* **1992**, *39*, 185−193.
(6) Spichiger, U. E.; Seiler, K.; Wang, K.; Suter, G.; Morf, W. E.; Simon, W. *Proc. SPIE* **1991**, *1510*, 118−130.
(7) Katerkamp, A.; Bolsmann, P.; Niggemann, M.; Pellmann, M.; Cammann, K. *Mikrochim. Acta* **1995**, *119*, 63−72.
(8) Kunz, R. E. *Sens. Actuators, B* **1997**, *38−39*, 13−28.
(9) Brecht, A.; Gauglitz, G. *Sens. Actuators, B* **1997**, *38−39*, 1−7.
(10) Bakker, E.; Lerchi, M.; Rosatzin, T.; Rusterholz, B.; Simon, W. *Anal. Chim. Acta* **1993**, *278*, 211−225.
(11) Shortreed, M. R.; Barker, S. L. R.; Kopelman, R. *Sens. Actuators, B* **1996**, *35−36*, 217−221.
(12) Demuth, C.; Spichiger, U. E. *Anal. Chim. Acta* **1997**, *355*, 259−268.
(13) Kawabata, Y.; Tahara, R.; Kamichika, T.; Imasaka, T.; Ishibashi, N. *Anal. Chem*. **1990**, *62*, 1528−1531.
(14) Citterio, D.; Rásonyi, S.; Spichiger, U. E. *Fresenius J. Anal. Chem*. **1996**, *354*, 836−840.
(15) Andres, R. T.; Sevilla, F. *Anal. Chim. Acta* **1991**, *251*, 165−168.
(16) Chau, L.-K.; Porter, M. D. *Anal. Chem*. **1990**, *62*, 1964−1971.
(17) Bürck, J.; Zimmermann, B.; Mayer, J.; Ache, H. J. *Fresenius J. Anal. Chem*. **1996**, *354*, 284−290.

10.1021/ac990156l CCC: $18.00
Published on Web 10/16/1999

Absorbance/transmittance optical sensors described to date have been criticized as they present short dynamic ranges, low sensitivity, or high response time and, as in the transmission mode, show interference effects (turbidity or sample matrix absorption) if radiation crosses the sample. However, direct absorbance/transmittance measurements are useful due to their broad applicability and versatility toward a large number of analytes. For this reason, we have designed and built a new integrated waveguide absorbance optode (IWAO) for chemical sensing based on radiation transmission through the core. The resulting optode aims at coupling the technological developments achieved by the communication industry in passive and active components for light transmission with the advantages of conventional spectroscopic techniques. The device consists of a microfabricated planar waveguide circuit, based on antiresonant reflecting optical waveguide structures (ARROW), and on a chemically active membrane, of a suitable thickness, deposited in a defined region of the former and yielding one part of the light guiding planar structure.

An ARROW is a planar waveguide in which light guidance is generated by an antiresonant reflection[18] in one of the directions. A multilayer structure is placed over the substrate in a way that a constructive interference in the reflected beam is produced for different conditions of incident light angle (~90°) and wavelength. Therefore, it can be stated that light is guided as single modal in the transversal direction to layers by (1) total internal reflection in the core on the core−upper cladding interface and by (2) antiresonant reflection on the core−substrate cladding interface due to this last interference cladding layer.

Concerning the transduction mechanism, it is established by absorbance/transmittance phenomena of the recognition optode membrane as it interacts with a given concentration of the analyte in the sample.

The membranes used in this system are the well-studied bulk optode membranes.[19−21] They contain a selective ionophore, a lipophilic ionic salt,[22−24] to maintain the electroneutrality, and a second ionophore with spectral change properties, denominated the chromoionophore or fluorophore (when fluorescence is the primary signal considered). Normally, this molecule is a pH indicator, whose spectral properties depend on the activity of the competing ions in the sample solution, the proton and the analyte. Such optodes rely on concentration changes within the bulk of the sensing membrane and follow the ion-exchange mechanism between the membrane and the aqueous solution. Assuming that no aggregates are formed, the overall extraction equilibrium for a potassium membrane can be formulated as a cation exchange between the bulk optode and the sample solution:

$$CH^+(org) + V(org) + K^+(aq) \overset{K_{exch}}{\rightleftharpoons} C(org) + KV^+(org) + H^+(aq)$$

The optode membrane senses potassium in an aqueous solution by extracting potassium ions into the membrane to form the positively charged complex with the ionophore used, valinomycin (V). To preserve electroneutrality in the membrane, the protonated chromoionophore (CH^+) sheds its proton to the aqueous phase and the measured absorbance decreases. More detailed mechanistic descriptions can be found in the literature.[25−27]

Therefore, simple sensing schemes can be designed following the optical response toward potassium activity and keeping constant the solution pH. This well-described bulk optode has been applied in this work to the planar waveguide device to validate its properties.

Obtained results demonstrate that this new approach represents an important advancement in the development of specific integrated absorbance optochemical sensors, with increased sensitivity and response times comparable to conventional membrane-based absorbance/transmission techniques.

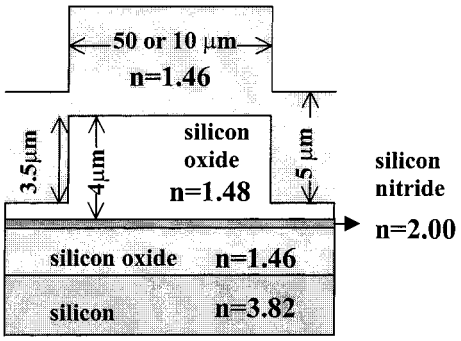

Figure 1. Rib ARROW structure cross section of the fabricated waveguide showing the different widths and refractive indexes of every silicon layer. The guided light zone in the waveguide core is also schematically shown as a white region.

EXPERIMENTAL SECTION

Device Fabrication. There are three differentiated regions in the IWAO: an input ARROW waveguide, an output ARROW waveguide, and a free propagation region, where the membrane is placed. The waveguides were constructed using complementary metal oxide semiconductor (CMOS)-[28,29] compatible processes over a silicon wafer. The transversal section of the ARROW waveguide is shown in Figure 1. The SiO_2 substrate−cladding layer was made by thermal oxidation of the silicon wafer. The Si_3N_4 ARROW layer was deposited using low-pressure chemical

(18) Benaissa, K.; Nathan, A. *Sens. Actuators, A* **1998**, *65*, 33−44
(19) Oesch, U.; Simon, W. *Anal. Chem.* **1980**, *52*, 692−700.
(20) Bakker, E.; Willer, M.; Lerchi, M.; Seiler, K.; Pretsch, E. *Anal. Chem.* **1994**, *66*, 516−521.
(21) Eugster, R.; Rosatzin, T.; Rusterholz, B.; Aebersold, B.; Pedrazza, U.; Rüegg, D.; Schmid, A.; Spichiger, U. E.; Simon, W. *Anal. Chim. Acta* **1994**, *289*, 1−13.
(22) Gehrig, P.; Morf, W. E.; Welti, M.; Pretsch, E.; Simon, W. *Helv. Chim. Acta* **1990**, *73*, 203-212.
(23) Schaller, U.; Bakker, E.; Spichiger, U. E.; Pretsch, E. *Anal. Chem.* **1994**, *66*, 391−398.
(24) Rosatzin, T.; Bakker, E.; Suzuki, K.; Simon, W. *Anal. Chim. Acta* **1993**, *280*, 197−208.
(25) Morf, W. E.; Seiler, K.; Lehmann, B.; Behringer, C.; Tau, S.; Hartman, K.; Sorensen, P. R.; Simon, W. *Ion-Selective Electrodes*; Pergamon Press: New York, 1989; Vol. 5, pp 115−131.
(26) Seiler, K.; Simon, W. *Sens. Actuators, B* **1992**, *6*, 295−298.
(27) Spichiger, U.; Simon, W.; Bakker, E.; Lerchi, M.; Bühlmann, P.; Haug, J. P.; Kuratli, M.; Ozawa, S.; West, S. *Sens. Actuators, B* **1993**, *11*, 1−8.
(28) Moreno, M.; Domínguez, C.; Muñoz, F.; Calderer, J.; Morante, J. R.; *Sens. Actuators, A* **1997**, *62*, 524−528.
(29) Moreno, M.; Garcés, I.; Muñoz, J.; Domínguez, C.; Calderer, J.; Villuendas, F.; Pelayo, J. *Advances in science and technology: advanced materials in optics, electrooptics and communication technologies*; P. Vinzencini: Faenza, Italy, 1995; Vol. 11, pp 465−472.

vapor depositions (LPCVD)[30] at a temperature of 800 °C. Upper cladding and core layers correspond to different stoichiometry silicon oxide layers deposited using plasma-enhanced chemical vapor depositions (PECVD)[30] at 300 °C. The rib structure and free propagation region were fabricated by reactive ion etching processes (RIE)[31] used in integrated optics.

Light guidance through the different layers can be explained in a summarized way as follows: light from a single-mode optical fiber at the operating wavelength is coupled to the input waveguide. Modal distribution in the input waveguide is single modal in both lateral and transversal directions, due to ARROW and rib structures. The rib structure generates an effective refractive index difference between the core area and its adjacent layers and guides light in the lateral direction, achieving single-mode behavior in this direction for a single waveguide width. Light exiting the input waveguide is coupled to the membrane, which is placed in the free propagation region. As the thickness of the membrane is designed to be the same as the height of the core, light remains guided in the transversal direction to the layers. The characteristics of the ARROW structure make it so that, as the refractive index of the membrane is near 1.46, the modal distribution of the light in the transversal direction will not change significantly. Therefore, light will remain guided in this direction in the membrane despite the use of aqueous solutions on the top of the waveguide or the occurrence of little changes in the refractive index of the membrane. To sum up, light is propagated inside the membrane and, at the same time is diffracted in the lateral direction because the rib structure is eliminated. The simulated behavior is shown in Figure 2. The output waveguide core, which is 4 μm high, has to be wider than the input waveguide to avoid high coupling losses of the diffracted and propagated light from the membrane.

The chip layout can be observed in Figure 3 where the narrow waveguide used for light input and the wider one used for light collection are clearly differentiated. The free propagation region is the space on the central area where the bulk optode is placed (Figure 3b). The design employed in this study incorporated a 0.5-mm-long cavity. Two similar waveguides were constructed at both sides of the device to verify the fabrication process and the light transmission. The device was finally cut to a 5 × 15 mm chip.

Figure 3c shows the experimental diffraction of the radiation in the membrane obtained with a 0.5-mm-long cavity. To enhance the performance of previously described devices, and therefore to simplify the operation, the input excitation waveguide and the collection waveguide were coupled to a 4-μm single-mode input fiber and a standard 50/125-μm multimode output fiber, respectively. This coupling was realized using optical-grade epoxy resin and a microfabricated V-grooved auxiliary support, also constructed in silicon (Figure 4).

Apparatus. Previous absorbance measurements for the PVC bulk optode characterization were done with a double-beam UV−visible−NIR scanning spectrophotometer (Shimadzu UV-3101PC) in a continuous-flow system using a conventional measurement cell, similar to others already reported.[32] Another flow cell was specially built to evaluate the IWAO in flow conditions. The design sought to minimize the dead volume and to prevent sluggish response times and long washout times. The final configuration was similar to the wall-jet layout flow cells. The flow system was completed with a Gilson Minipuls 3 peristaltic pump equipped with Tygon pump tubing. A six-port distribution valve (Rheodyne 5012, Cocati, CA) was used for the selection of the standard solution. The flow rate used was 3 mL/min. Flow lines were build using PTFE 0.8-mm-inner diameter tubing. The optical source was an LED laser (GCA Fiberoptics, GCA-3200-FC-08-Z) emitting at 670 nm with 20-nm spectral width, coupling 1-μW optical power to the device. Fiber-emitter and fiber-detector coupling was done with standard optical fiber connectors. The detector was a PIN photodiode connected to a transimpedance preamplifier. The signal was amplified and filtered using a lock-in amplifier (SR810 DSP Stanford Research Systems) that also tuned the modulation frequency of the LED source (1.1 kHz). The described experimental setup is presented in Figure 5.

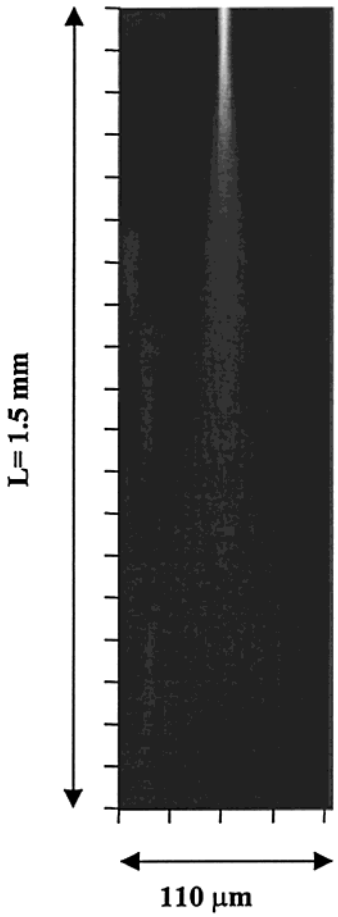

Figure 2. Simulation of the light propagation within the optical membrane in one of the constructed devices featuring a 1.5-mm-length free propagation region.

Reagents. Aqueous solutions were prepared with doubly distilled water, potassium chloride (Merck, Darmstadt, Germany), and magnesium acetate (Panreac, Barcelona, Spain). Salts were of the highest purity available. The standard solutions were

(30) Moreno, M.; Muñoz, J.; Garrido, B.; Samitier, J.; Calderer, J.; Domínguez, C. *Advances in science and technology: advances in inorganic films and coatings*; P. Vinzencini: Faenza, Italy, 1995; Vol. 5, pp 149−154.

(31) Domínguez, C.; Muñoz, J.; González, R.; Tudanca, M. *Sens. Actuators, A* **1993**, *37*−*38*, 779−783.

(32) Dinten, O.; Spichiger, U. E.; Chaniotakis, N.; Gehrig, P.; Rusterholz, B.; Morf, W. E.; Simon, W. *Anal. Chem.* **1991**, *63*, 596−603.

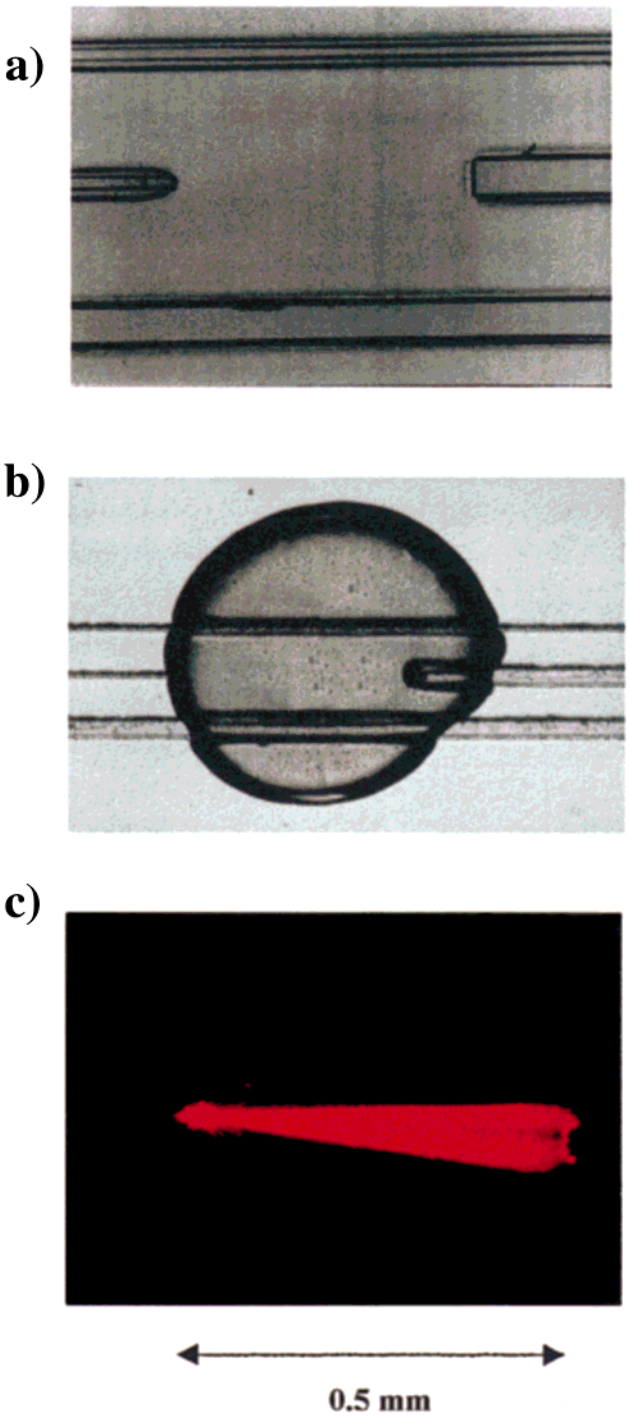

Figure 3. (a) Upper close-up view of one of the built sensors. The length of the free propagation region, the input, and the collection waveguide can be noticed. (b) Outline of the optical membrane (bulk optode) as it appears after deposition. (c) Radiation transmission in a free propagation region length of 0.5 mm.

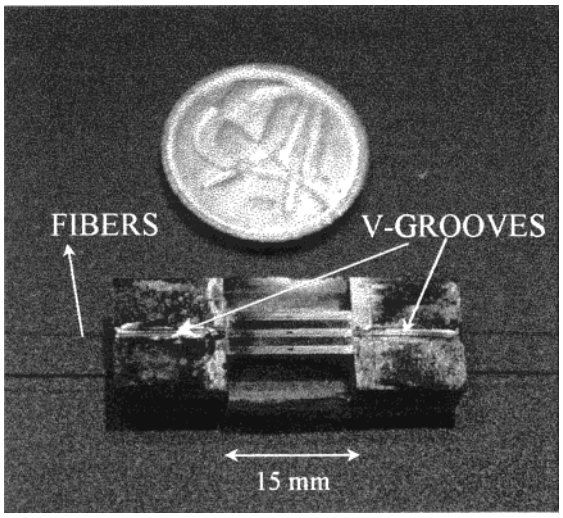

Figure 4. Prototype of the integrated waveguide optode connected with optical fibers to the light source and the detector. The fibers were coupled to the planar waveguides with the aid of a V-grooved support.

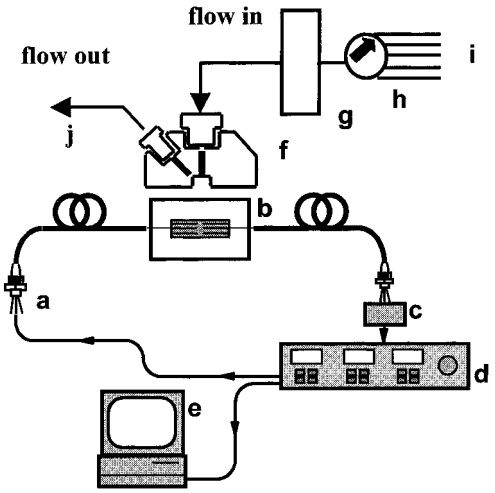

Figure 5. Experimental setup used in the measurements: (a) LED laser source, (b) IWAO, (c) silicon photodetector, (d) lock-in amplifier, (e) data acquisition computer, (f) measurement cell, (g) peristaltic pump, (h) selection valve, (i) samples, and (j) waste.

prepared from a 1 M KCl stock solution in 0.05 M acetic acid/magnesium acetate buffer at pH 5.5 with serial dilutions using the specified buffer. For membrane preparation, the following components were obtained from Fluka (Buchs, Switzerland): poly(vinyl chloride) (PVC high molecular weight) as the polymer, bis(2-ethylhexyl) sebacate (DOS) as the plasticizer, and tetrahydrofuran (THF) as the solvent; potassium tetrakis(4-chlorophenyl)borate (KTpClPB) was used as the lipophilic ionic salt, valinomycin as the potassium selective ionophore, and lipophilized Nile Blue (ETH 5294) as the chromoionophore.

Experimental Procedures. *Membrane Preparation and Characterization*. The membrane components were weighed out and dissolved in 1.5 mL of THF to prepare the cocktail solution, the composition of which was as follows: 0.5 wt % ETH 5294, 1.0 wt % valinomycin, 0.5 wt % KTpClPB, 31.0 wt % PVC, and 67.5 wt % DOS.[6] To obtain a thickness of 4 μm, a spin-on device was used at 2000 rpm to deposit 100 μL of this cocktail over microscope slides. These, once cut, were enclosed in pairs in the measurement cell for the purpose of spectroscopic characterization of the sensing membrane. To characterize the IWAO, 10 μL of a diluted cocktail (1:3) in THF was dropped onto the previously silanized, free propagation region of the device defined between the input and output rib ARROW structures, maintaining a THF environment to provide slow evaporation. After THF evaporation, membranes with a homogeneous thickness of 4 μm were obtained. The thickness of membranes was measured using confocal microscopy.[33]

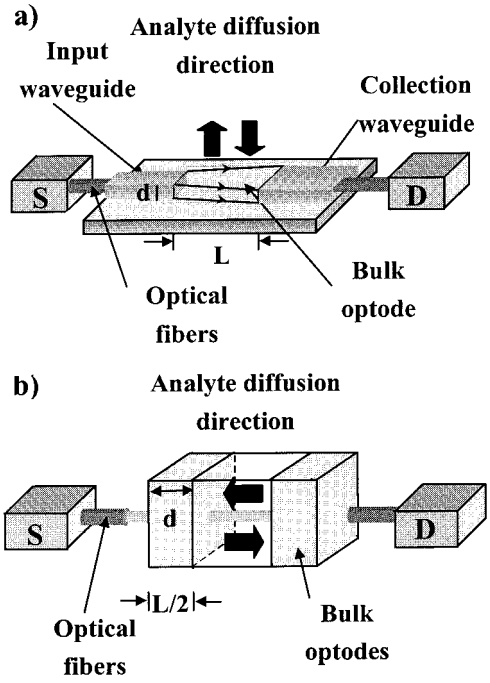

Figure 6. General schematic comparison of both absorbance optodes: (a) New IWAO, in which light travels perpendicularly to the diffusion direction, making the path length independent of the membrane thickness. *L*, path length. (b) Conventional absorbance device (transmission/reflection mode), in which the path length corresponds to the membrane thickness. 2*d*, path length. S, light source; D, detector.

Silanization Procedure. Silicon surface silanization was done with 3-(trimethoxysilyl)propyl methacrylate (Fluka) dissolved in toluene (Panreac) (10:90). The main objective was to enhance the adherence of the hydrophobic PVC membranes.[34] Different volumes of the silanization mixture were dropped over the surface in a dry atmosphere. After this step, the IWAO was placed in an oven at 40 °C for 1 h and then cleaned and dried with acetone.

RESULTS AND DISCUSSION

General Features of the New Absorbance/Transmittance Sensor. The novel sensor was conceived to optimize four essential characteristics that define a high-quality optochemical sensor: *enhanced and sizable sensitivity* (depending on the free propagation region length), an *adequate selectivity* toward a certain analyte (regulated by the ionophore), *low response time*, and *minimization of interference effects* caused by the solution matrix. To attain these goals, we propose a basic structure composed of a single-mode integrated optic waveguide (as the input waveguide), a bulk optode (as the recognition region), and a wider multimode waveguide (as the collection waveguide) in a continuous arrangement. It is displayed in Figure 6a. The input and output waveguides are rib ARROW structures made by dielectric materials compatible with the standard integrated circuit and micromachining technology.

The use of ARROW structures in absorbance-based optical sensors offers some advantages: (1) As the field distribution in the transversal direction is equivalent to a 4-μm-thick single-mode waveguide, they can be efficiently coupled to single-mode fibers[35] and minimum insertion losses can be achieved (15 dB). (2) They show high tolerance to variations in the fabrication parameters because they present a single modal distribution despite changes in the refractive index of the core. This is due to the interference filter effect of the antiresonant layers that attenuates higher order modes. (3) ARROW structures are technologically easier to fabricate than conventional waveguides, and therefore, less costly and more robust fabrication processes are implied. The reason is that conventional waveguides must have much thicker substrates (~10 times thicker) to obtain similar radiation losses in the substrate. (4) Using 4-μm-thick core waveguides, it is possible to deposit thin membranes that act as waveguides in the transversal direction. Conventional waveguides present a thinner core thickness to achieve a single-mode behavior in the transversal direction (typically hundreds of nanometers), so they are less suited for sensor construction. (5) Cutting the input waveguide to deposit the sensing membrane and collecting light after its propagation is only possible with ARROW configurations. In a conventional waveguide, the membrane refractive index must remain higher than the surrounding media to allow guidance in the transversal direction and to avoid light radiation into the substrate. For this kind of waveguide, it is a critical issue because the real part of the refractive index of the membrane changes together with the imaginary part.[36] Additionally, in a conventional single-mode waveguide, the refractive index of the core and cladding regions should remain very close. Therefore, there will be high losses in the membrane region if its refractive index changes to a lower value than the refractive index of the substrate.

On the other hand, the main improvement achieved is that ARROW structures allow light to travel in the transversal direction to the mass transfer, rendering the response time independent from the light path length. Therefore, it is possible to increase the sensitivity without enlarging simultaneously the time needed to achieve the steady-state signal. This effect can be understood if we consider that, in the IWAO, the membrane thickness do not spatially define the light path length as it is only limited by the length of the free propagation region. Figure 6 illustrates this concept by comparing the proposed design (Figure 6a) with the conventional bulk optode configuration (Figure 6b). In the IWAO, the free propagation region length (*L*) can be easily enlarged, and therefore, it is possible to obtain a sensitivity increase while the membrane thickness (*d*) remains unaltered and the response time unmodified.

Moreover, light has no interaction with the sample solution, and interference due to the sample matrix (absorbance or turbidity) is avoided. This conclusion can be theoretically demonstrated with simple calculations based on light transmission in planar waveguides.[37] If the membrane and the solution have a refractive index of 1.46 and 1.33, respectively, then 99.77% of the optical power is enclosed in the membrane and the remaining 0.23% is guided outside (the evanescent field). Changing the

(33) Artigas, R.; Pintó, A.; Laguarta, F. *Proc. SPIE* (Symposium Laser Metrology and Inspection), in press.
(34) Yamauchi, S. *Chemical Sensor Technology*; Elsevier: Tokyo, 1992; Vol. 4, Chapter 3.
(35) Garcés, I.; Villuendas, F.; Vallés, J.; Domínguez, C.; Moreno, M. *J. Lightwave Technol.* **1995**, *14*, 798−815.
(36) Freiner, D.; Kunz, R. E.; Citterio, D.; Spichiger, U. E.; Gale, M. T. *Sens. Actuators, B* **1995**, *29*, 277−285.
(37) März, R. *Integrated Optics: Design and Modeling*; Artech House Publishers: Boston, 1994; Chapter 3.

refractive index of the solution from 1.33 to 1.36, 99.71% of the optical power is guided in the membrane. On the other hand, if the refractive index of the membrane vary from 1.46 to 1.47 and considering and external index of 1.33, 99.79% of the power is guided in the membrane. Therefore, it can be assumed that the guided field in the membrane is almost independent of refractive index variations of the solution and the membrane.

Recently, the idea on which the IWAO sensor is based has also been exploited in planar configurations. So, other approaches have been proposed to attain similar objectives, but the optical phenomena used or the integration of the sensing layer to the guiding elements is somewhat different from the design presented here. Two of them use the evanescent field: with an identical membrane[38] or with membranes of different nature[39] deposited over standard glass substrates. Another approach employs capillary optical sensors.[40] A further design[41] consists of measurements of changes in the core, very similar to the optical sensor presented in this paper. However, it requires a complex optical setup in contrast with our simple integrated optical configuration. This complexity hinders future developments and applications. Additionally, this device shows high light losses, requiring the use of powerful emission sources that increase instrumental costs. An added disadvantage is that the high-intensity light sources used may cause the photobleaching of membrane components.

Spectroscopic Evaluation Results. To demonstrate the possibilities of this novel sensor, we constructed a microfabricated absorbance-sensing device selective to potassium ion, activated with the well-known potassium bulk optode.[42] Optical membranes were characterized initially with a conventional absorbance/transmittance flow cell in a continuous-flow system. These data were also useful for comparison purposes. Figure 7 shows the absorption spectra of a membrane when the potassium concentration in a constant pH was varied and where the absorption maximum of the chromoionophore used (the lipophilized Nile Blue derivative) is clearly observed at 660 nm. In this case, a conventional light source coupled to a monochromator was used to follow the response with time at different analyte concentrations. The membrane in contact with a 0.1 M potassium hydroxide solution was used as the reference signal in all cases. All the parameters determining the membrane response were optimized in order to guarantee the same operational conditions, using the conventional technique as well as the integrated waveguide absorbance sensor. The buffer concentration chosen was 0.05 M. The measuring ranges of these optodes typically cover from two to four concentration decades and depend on the membrane composition and the buffer pH. As it is known, the concentration range can be shifted within a wide range by changing the buffer pH, as it determines the quantity of available protons.[43] In our study, the pH selected was 5.5 to cover the range from 1×10^{-4} to 1×10^{-1} M potassium concentrations.

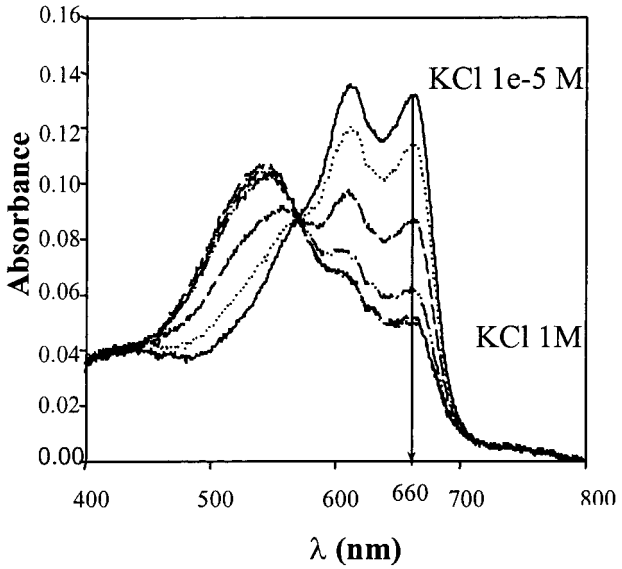

Figure 7. Changes in the absorption spectra of the potassium bulk optode membrane, incorporating the lipophilized Nile Blue chromoionophore. Each spectrum was acquired after the steady state was attained. The maximum absorption band of the protonated form in the membrane can be observed at the 660-nm wavelength.

To make an appropriate comparison between response times, the thickness of the bulk membranes used in both systems was the same. This fact implied that the conventional device, which contained two membranes, had a path length corresponding to twice the thickness of each membrane. Two representative calibration experiments obtained with both devices are shown in parts a and b of Figure 8. They demonstrated the fact that the sensitivity of the IWAO was much higher although the conventional device had a larger total membrane thickness. Whereas the total absorbance change in the conventional configuration was 0.05 AU, the total absorbance change achieved using the IWAO was 3.49 AU. As can be observed, the great advantage offered by the IWAO is the possibility of obtaining high sensitivity without raising the chromoionophore ratio, which generates solubility problems in the membrane, and without increasing the membrane thickness that leads to high response times. This fact could be theoretically explained if it is assumed that diffusion controls the response rate when thick membranes are used and when the Nernst layer is thin. The 95% response time could be approximated to[44]

$$t_{95\%} = 1.13(d^2/D_m)\ (\mathrm{s}) \qquad (1)$$

where D_m is the mean diffusion coefficient in the membrane phase (cm^2/s) and d is the diffusion layer thickness (cm). This thickness is equivalent to the path length in the case of the conventional device. For the proposed IWAO, the free propagation region length between the input and the output waveguides (see Figure 6a,b) determines the optical path length.

The dynamic range considered was from 1×10^{-4} to 1 M KCl concentration range using the IWAO, similar to that obtained with the conventional configuration (1×10^{-5}–1×10^{-1} M); see Figure 9.

(38) Tóth, K.; Nagy, G.; Lan, B. T. T.; Jeney, J.; Choquette, S. J. *Anal. Chim. Acta* **1997**, *353*, 1−10.
(39) Saavedra, S.; Yang, L. *Anal. Chem.* **1995**, *67*, 1307−1314.
(40) Weigl, B. H.; Wolfbeis, O. S. *Anal. Chem.* **1994**, *66*, 3323−3327.
(41) Hisamoto, H.; Kim, K.; Manabe, Y.; Sasaki, K.; Minamitani, H.; Suzuki, K. *Anal. Chim. Acta* **1997**, *342*, 31−39.
(42) Wang, K.; Seiler, K.; Morf, W. E.; Spichiger, U. E.; Simon, W.; Linder, E.; Pungor, E. *Anal. Sci.* **1990**, *6*, 715−720.
(43) Bakker, E.; Bühlmann, P.; Pretsch, E. *Chem. Rev.* **1997**, *97*, 3083−3132.
(44) Seiler, K. *Ion-Selective Optode Membranes*; Fluka Chemie AG: Buchs, Switzerland, 1993; Chapter 4.

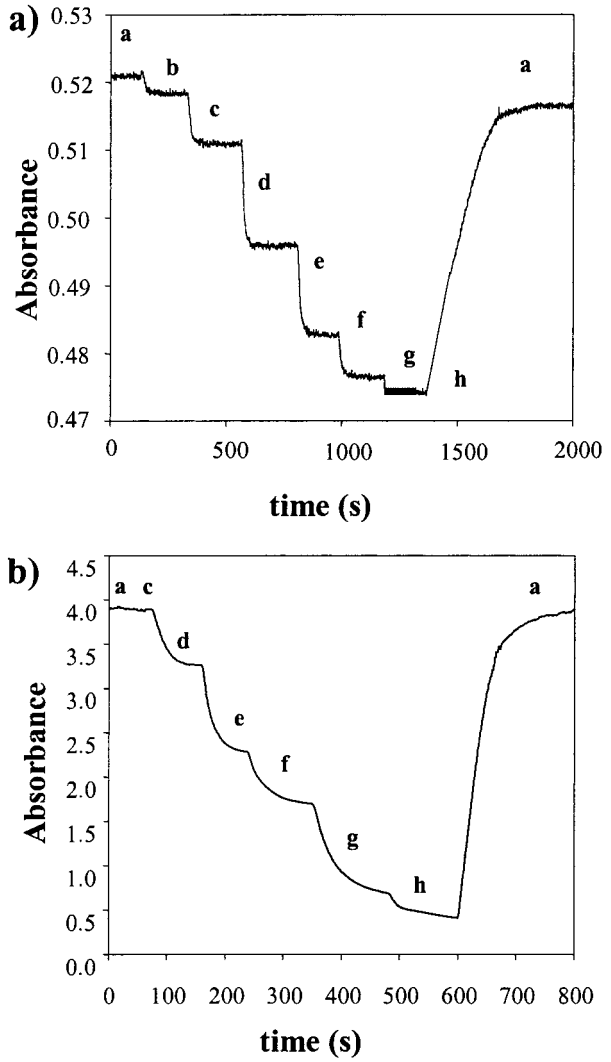

Figure 8. Calibration experiments with both configurations: (a) Conventional absorbance device; (b) IWAO. The recordings of absorbance versus time show the attainment of the steady-state signal. Potassium chloride solutions: (a) buffer, (b) 1×10^{-5} M, (c) 1×10^{-4} M, (d) 1×10^{-3} M, (e) 1×10^{-2} M, (f) 1×10^{-1} M, (g) 5×10^{-1} M, and (h) 1 M.

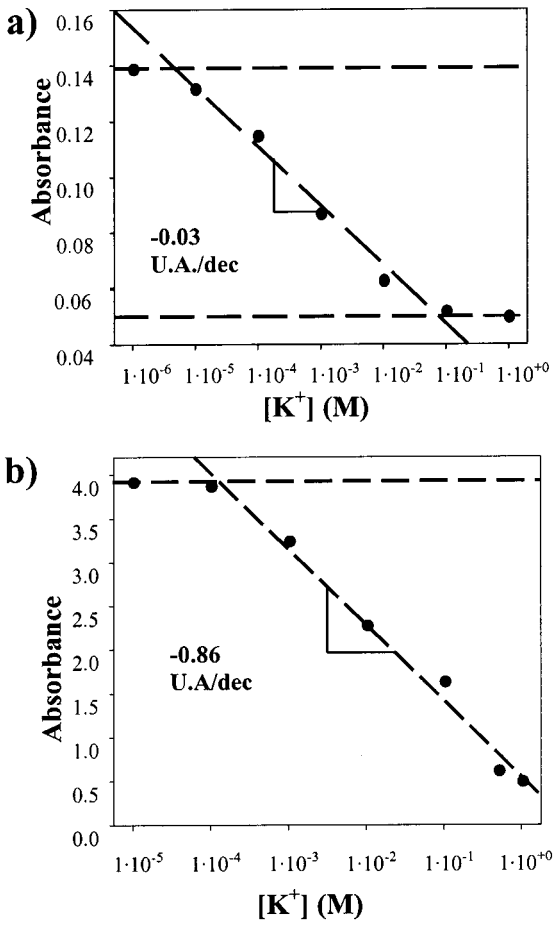

Figure 9. Calibration curves showing the absorbance response versus potassium concentration: (a) Conventional absorbance device (bulk optode); (b) new IWAO. Each point corresponds to the steady-state reading, with different potassium chloride solutions (pH buffered at 5.5 with 0.1 M magnesium acetate).

Table 1. Comparison Table of Response Features of the IWAO Sensor

	absorbance change (AU)		response time[a] ($t_{90\%}$) (min)	
step change (M)	conventional configuration	IWAO	conventional configuration	IWAO
buffer−1×10^{-5}	0.008	0	0.97	
1×10^{-5}−1×10^{-4}	0.009	0.049	0.85	
1×10^{-4}−1×10^{-3}	0.021	0.628	1.20	0.29
1×10^{-3}−1×10^{-2}	0.018	0.976	1.17	0.16
1×10^{-2}−1×10^{-1}	0.009	0.642	1.00	0.52
1×10^{-1}−5×10^{-1}	0.001	1.010	0.43	0.54
1−buffer	0.062	3.490	11.13	1.76

[a] Response times are calculated as the time when 90% of the final response is attained after the step change for both sensing modes.

To compare results, the response time was evaluated by the fit of an exponential decay to every concentration change. Since the equilibrium must be reached for every measurement, the decay model used was

$$A = A_o + be^{-c\Delta t}$$

where c and b are two constants, Δt is the elapsed time in seconds, and A_o is the final signal. Considering the boundary conditions, the step start when $\Delta t = 0$ and $A = A_o + b$; the steady-state with $\Delta t = \infty$, $A = A_o$, the 90% response time can be formulated as

$$\Delta t_{90\%} = -(\ln 0.1/c) \qquad (3)$$

The response time values and the absorbance changes for different concentration steps are presented in Table 1. The absorbance change achieved with the conventional configuration was multiplied using the IWAO almost for every step change, while the response times for both devices were comparable. If linearity is assumed, a simple calculation considering an IWAO path length (L) of 0.5 mm permits to predict a 100-fold sensitivity increase in comparison with the 8 μm path length of the conventional device. This parameter (L) was fixed during the fabrication process according to the predicted sensitivity because there is a maximum allowed length, which basically depends on

the optical properties of the polymer and on the width of the collection waveguide.

CONCLUSIONS

An IWAO was developed. It is based on a planar microoptical circuit where an optically sensitive membrane acts as the recognition region as well as the guiding sensor element. This IWAO confines the light in the perpendicular direction to the mass transfer and is confirmed to be a useful tool to solve some drawbacks typical to conventional absorbance optochemical sensors. Short response times are achieved since thin membranes are used while long path lengths can be designed to provide large sensitivities. On the other hand, interference effects brought by the solution matrix are expected to be minimized because the light does not propagate in this external medium (only 0.23% of the optical power has been calculated as the evanescent field). For these reasons, the IWAO is a very promising device, with large applicability that adapts existing absorbance schemes to the design and construction of novel specific optochemical sensors.

Some prototypes were fabricated and characterized by adapting potassium-selective optode membranes and the results obtained confirmed the expected behavior.

Optimized designs for specific applications could be developed if other refractive or reflective planar components, including different waveguides, are used. Different propagation lengths and, as a result, various sensitivities and dynamic ranges can be achieved. Different optode configurations could be built; reference signal or multiple specific sensors can be implemented in a chip using suitable bidimensional circuits.

Furthermore, the study and optimization of new membrane compositions is in progress. Some dyes applicable to the NIR region, where inexpensive and efficient commercial LED lasers are available, are being characterized for use in this IWAO.

ACKNOWLEDGMENT

Spanish CICYT agency (through Projects TIC93-0525 and TIC97-0594-C04-02) is greatly acknowledged for financial support of the present work.

Received for review February 10, 1999. Accepted August 11, 1999.

AC990156L